Esther Santos*, Enrique Rodríguez-Fernández, Clara Casado-Coterillo and Ángel Irabien

Hybrid Ionic Liquid-Chitosan Membranes for CO_2 Separation: Mechanical and Thermal Behavior

Abstract: Pure chitosan (CS) and hybrid ionic liquid-chitosan membranes loaded with 5 wt% 1-ethyl-3-methylimidazolium acetate ([emim][Ac]) ionic liquid were prepared in order to improve the thermal behavior of supported ionic liquid membranes (SILMs) for CO_2 separation. Gas permeability, solubility and diffusivity were evaluated in the temperature range 298–323 K. The temperature influence was well described in terms of the Arrhenius–van't Hoff exponential relationships. Activation energies were calculated and compared with those obtained for SILMs with the same ionic liquid. The introduction of this ionic liquid in the hybrid solid membrane decreases the permeability activation energy, leading to a lower influence of the temperature in the permeability and diffusivity. Moreover, the thermal behavior is similar to pure chitosan membranes, and the mechanical strength and flexibility were improved due to the introduction of the ionic liquid in the polymer matrix.

Keywords: green chemistry, chitosan, ionic liquid, CO_2/N_2 separation, hybrid membranes

1 Introduction

The ability to efficiently separate CO_2 from other light gases has received a great attention aiming at capture greenhouse gases. Even though existing commercial CO_2

*Corresponding author: Esther Santos,** Department of Chemical and Biomolecular Engineering, ETSIIyT, Universidad de Cantabria, Avda. Los Castros s/n Santander 39005, Spain, E-mail: santosse@unican.es
Enrique Rodríguez-Fernández, Department of Chemical and Biomolecular Engineering, ETSIIyT, Universidad de Cantabria, Avda. Los Castros s/n Santander 39005, Spain, E-mail: erf16@alumnos.unican.es
Clara Casado-Coterillo, Department of Chemical and Biomolecular Engineering, ETSIIyT, Universidad de Cantabria, Avda. Los Castros s/n Santander 39005, Spain, E-mail: clara.casado@unican.es
http://orcid.org/0000-0002-4454-7652
Ángel Irabien, Department of Chemical and Biomolecular Engineering, ETSIIyT, Universidad de Cantabria, Avda. Los Castros s/n Santander 39005, Spain, E-mail: angel.irabien@unican.es

capture facilities are based on wet scrubbing using aqueous amine solutions [1], both organic and inorganic membranes have been developed due to the simplicity of the process, the modularity of the permeation unit and the development of novel tailor-made membrane materials for specific gas separations [2]. Permeability and selectivity are the fundamental parameters characterizing the gas separation using membrane-based technologies. There is a general trade-off between both parameters described by the upper bound reported by Robeson in 2008 [3].

One of the ways of enhancing the CO_2 permeability and selectivity is based on the use of room temperature ionic liquids (RTILs). RTILs are liquid salts at room temperature, typically composed of bulky organic cations and organic or inorganic anions showing a large variety of properties such as negligible vapor pressure, thermal stability at high temperatures or non-flammability [4]. Additionally, their physicochemical properties can be tuned by the appropriate selection of the cation or anion resulting in enhanced properties such as gas solubility. It is reported in literature that RTILs with acetate anions show very high CO_2 solubility [5].

The permeability of CO_2 and N_2 through RTILs has been studied in the form of supported ionic liquid membranes (SILMs) by pouring selected RTILs in a porous commercial support [6]. In a previous work [5], the CO_2/N_2 separation in the temperature range 298–333 K of commercial acetate-based RTILs and ionic monomers was studied in the form of SILMs. The temperature influence on the gas permeability, solubility and diffusivity was evaluated and the activation energies were calculated but the long-term stability was not evaluated. The main drawback of SILMs is the membrane stability, which is still a pending issue. Mixed-matrix membranes (MMMs) are explored as a means of combining synergic effects of the dispersed phase or filler and a permeable and easy processability of a polymer to improve membrane fabrication and performance [7]. There are examples in the literature of hybrid polymer + RTIL for pervaporation [8] and MMMs for gas separation based on polymer + RTIL + SAPO-34 zeolite and ZIF-8 porous materials [9, 10]. However, from our knowledge, it is the first time a completely solid membrane based on hybrid

acetate-based RTIL + biopolymer materials for CO_2/N_2 separation is reported in the literature.

The biopolymer chosen is semi-crystalline chitosan, which is a deacetylated derivative from chitin, the second most abundant natural polymer, cheap and obtained from renewable sources. Chitosan membranes have been studied for the separation of CO_2/N_2 up to 423 K [11].

In this work, a small amount of acetate-based [emim][Ac] ionic liquid is embedded into chitosan matrix to provide a new hybrid solid membrane with improved CO_2/N_2 separation properties. CO_2 permeability, solubility and diffusivity at 298−323 K are studied and the thermal and mechanical behavior is evaluated.

2 Materials and methods

2.1 Materials

Chitosan (**CS**; coarse ground flakes and powder, Sigma-Aldrich) with a deacetylation degree higher than 75 wt% and high viscosity in 1 wt% acetic acid/water was used as purchased. Glacial acetic acid was purchased from Panreac. 1-ethyl-3-methylimidazolium acetate, [emim][Ac] (**RTIL**, assay ≥96,5%, $C_8H_{14}N_2O_2$ CAS No. 143314-17-4) was supplied by Sigma Aldrich and used without further purification. Their main properties including their molecular structure, molecular weight, density and degradation temperatures are listed in Table 1. The gases used in the experiments were carbon dioxide (99.7 ± 0.01 vol %) and nitrogen (99.999 ± 0.001 vol %) provided by Air Liquide (Spain).

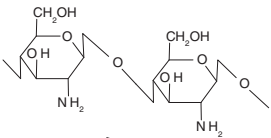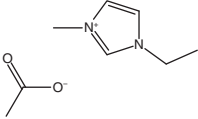## 2.2 Synthesis of membranes

In this work, we prepared dense membranes by solution casting in a similar method as previously reported [12, 13].

In a typical synthesis, CS 2 wt% solution was prepared by dissolving the polymer in 2 wt% acetic acid/water solution and stirred at 353 K for 24 h under reflux conditions. The CS solution obtained was filtered to remove insoluble impurities and degassed in ultrasonic bath for about 15 min before casting approximately 10 mL of solution on a polystyrene Petri dish and evaporating at room temperature for 2−3 days. CS membranes were then removed from the Petri dish. The membrane was then neutralized in 1 M NaOH and rinsed with abundant distilled water and dried at 277 K before CO_2 and N_2 permeation experiments in order to ion-exchange the functional groups of the polymer matrix as depicted in Table 1. RTIL/CS membranes were prepared with a nominal 5 wt% RTIL loading with respect to chitosan. In a typical synthesis: 0.042 g of RTIL was added to the 10 mL CS solution and stirred overnight before casting the same way as the pure polymer membranes.

2.3 Characterization methods

The experimental setup used for the gas permeation experiments has been previously described elsewhere [5]. A schematic diagram of the gas permeation unit is shown in Figure 1. In a typical experiment, the membrane is placed inside a stainless steel permeation cell, which provides an effective membrane area of 14.05 cm^2. The feed gas is introduced in the feed and permeate compartments through valves V1 and V2 for a few minutes till they are equilibrated. Then the permeate outlet is open (V4) to establish the driving force through the membrane. Two pressure transducers (Omega, UK) measure the pressure in the feed at the beginning and across the membrane during the experiment. The permeability values were calculated from the slope of the curve, at a pressure difference around 0.5 bar [14]. The influence of temperature was studied in the range from 298 to 323 K using a water bath keeping the process at isothermal conditions.

Table 1: Main characteristics of the studied materials.

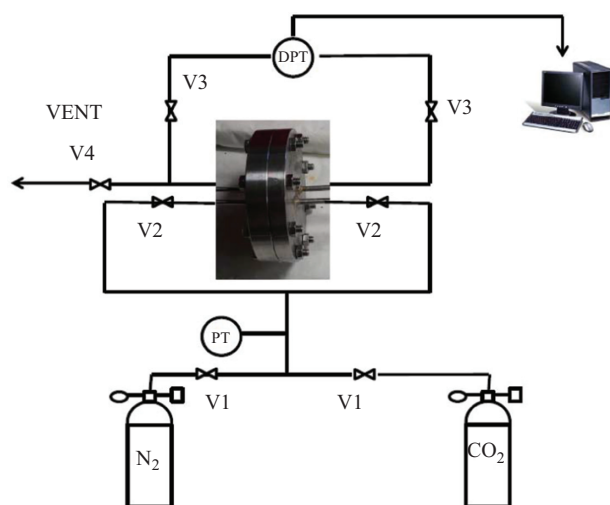| Materials	Molecular structure	Molecular weight (g mol^{-1})	Density (g cm^{-3}, 298 K)	T_{onset} (K)
CS		−	1.43	870
IL		170.21	1.098	481.4

Figure 1: Permeation unit for the CO_2/N_2 separation.

Gas diffusivity was calculated using the constant volume method, as reported in literature [13, 15]. Gas solubility was evaluated using a TGA-60H Shimadzu thermo balance where simultaneous TG/DTA analyses were performed. A molecular sieve trap was installed to remove traces of water from the feed gas. The sample temperature was measured with an accuracy of ± 0.1 K and the TG sensitivity was about 1 μg. The experimental conditions were a gas flow rate of 50 mL min⁻¹, temperatures from 298 to 323 K and atmospheric pressure. Thermal analyses were carried out in air atmosphere at temperatures ranging from room temperature to 973 K with a heating rate of 10 K min⁻¹. Mechanical stability tests were performed in a Zwick/Roell Universal Testing Machine with a head load up to 2.5 kN and 5 mm min⁻¹ under the following conditions: sample width 5 mm, grip to grip distance 40.20 ± 8.76 mm. The tensile strength and the elongation at break were averaged to 5–10 samples.

3 Theory

Gas permeability through the membrane was determined according to eq. (1) [16]:

$$\frac{1}{\beta} \cdot \ln\left(\frac{[p_{\text{feed}} - p_{\text{perm}}]_0}{[p_{\text{feed}} - p_{\text{perm}}]}\right) = \frac{1}{\beta} \cdot \ln\left(\frac{\Delta p_0}{\Delta p}\right) = P \cdot \frac{t}{\delta} \quad (1)$$

where p_{feed} and p_{perm} are the pressures in the feed and permeate compartments, respectively; β a geometric parameter (1,100 m⁻¹); P the permeability through the membrane calculated under constant partial pressure

difference; t the time and δ the membrane thickness. The ideal selectivity can be calculated as the ratio between the permeabilities of the two pure different gases.

The geometric parameter β (m⁻¹) is calculated from the membrane effective area and the volumes of feed and permeate compartments as follows [16]:

$$\beta = A_m\left(\frac{1}{V_{\text{feed}}} + \frac{1}{V_{\text{perm}}}\right) \quad (2)$$

where A_m is the membrane area (m²) and V_{feed} and V_{perm} are the volume of the feed and permeate compartments (m³) respectively.

The separation ability of a dense polymeric membrane is determined by the ideal selectivity, which is usually defined as the ratio of the single gas permeation of the components, i.e. CO_2 and N_2, in this work.

The permeability is a function of the absolute temperature and it is described in Arrhenius form [17]:

$$P = P_0 \exp(-E_p/RT) \quad (3)$$

where P_0 is the pre-exponential factor and E_p the activation energy of permeation.

The solubility can be related to the temperature by the van't Hoff equation [17]:

$$S = S_0 \exp(-\Delta H_s/RT) \quad (4)$$

where S_0 is the pre-exponential factor and ΔHs is the partial molar enthalpy of adsorption.

The gas diffusivity also follows the Arrhenius model [17]:

$$D = D_0 \exp(-E_D/RT) \quad (5)$$

where D_0 is the pre exponential factor and E_D the activation energy of diffusion.

4 Results and discussion

The elasticity and rigidity of the materials influence the mechanical resistance of the membranes. The tensile strength and elongation at break of the membrane materials under study are plotted in Figure 2. The tensile strength of the hybrid RTIL/CS membrane is lower than the pure polymer membrane, but the elongation at break is greatly improved, even higher than other data for CS-based membranes reported in the literature [18, 19]. This agrees with reported literature on chitosan-based membranes [20] and proves the physically observed flexibility of the novel hybrid membrane material.

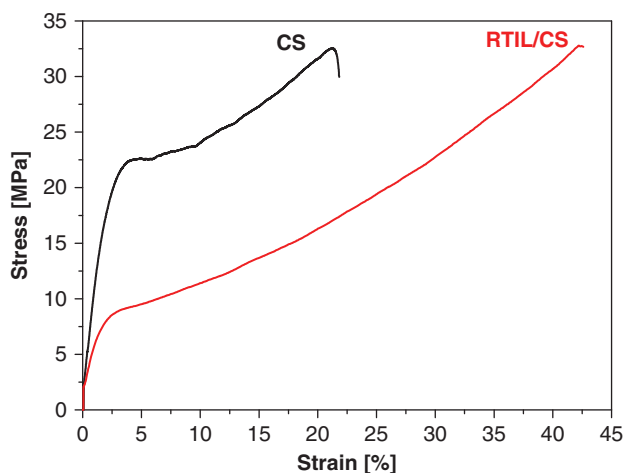Before analyzing the influence of temperature on permeation, the membrane thermal stability was

Figure 2: Mechanical properties of CS-based membranes.

measured by Thermo Gravimetric Analysis (TGA). Thermal degradation of CS and hybrid RTIL/CS membranes was examined in the range 298–973 K and the TGA curves are represented in Figure 3. The differential thermal analytical curve (DTA) is presented in the inset. The decomposition of chitosan powder agrees with literature [21]. The degradation of CS membranes involves the usual three stages: a first step up to 473 K for the evaporation of residual water in the membrane, composed of free water and bound water due to the hydrophilic nature of this biopolymer [22]; a second step from 473 to 823 K for the deacetylation and depolymerization of CS, since

RTIL is degraded at 473 K, and a third step for the final oxidation of the dense organic membrane (823–973 K). The pristine CS membrane has almost the same decomposition temperature as the precursor CS powder as it can be observed in the DTA inset in Figure 3. In the case of the RTIL, the thermal behavior is improved when comparing the pure component with the hybrid membrane. Although the thermal decomposition of pure CS and RTIL/CS membranes starts at similar temperatures, there is a slight shift to the right of 293 K in the second peak of the DTA curve introduced as inset.

Gas permeability increases with decreasing CO_2/N_2 selectivity, but the permselectivity of the RTIL/CS hybrid membrane is better than that of the pure CS membrane, which agrees with literature in ionic liquid-polymer membranes [9, 10]. The permeability obtained for CS and RTIL/CS membranes in this work is plotted against the Robeson's upper bound in Figure 4 [3]. The CO_2 permeability of pure CS membranes decreases from 393 to 307 Barrer, while the permeability through RTIL/CS membranes increases from 1,293 to 1,338 Barrer, when working temperature is increased from 298 to 323 K. The ideal selectivity of pure CS membranes decreases with temperatures from 1.5 to 0.5, because the increase in diffusivity is lower than the decrease of solubility with increasing temperature. In contrast, the influence of temperature on the performance of hybrid RTIL/CS membranes tends to disappear when RTIL is introduced in
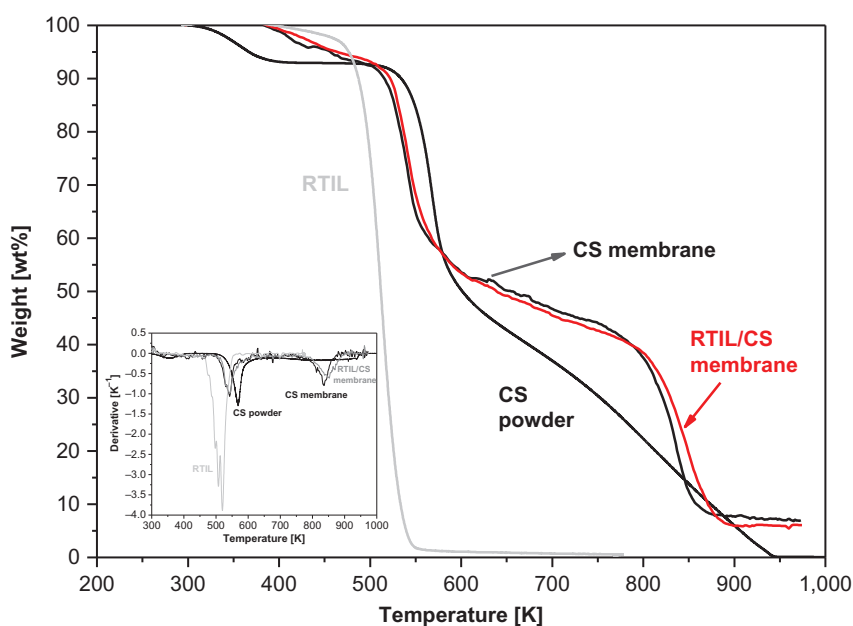

Figure 3: TGA curves of the CS and hybrid RTIL/CS membranes. TGA of CS powder and [emim][Ac] RTIL are also included for comparison.
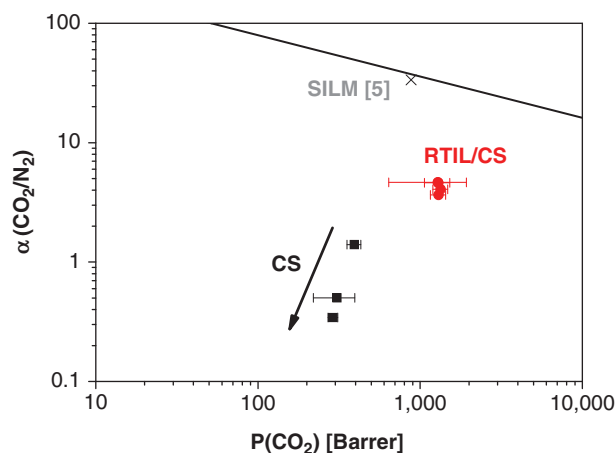
Figure 4: Robeson's upper bound for CO$_2$/N$_2$ separation with the permeability values of CS and IL/CS membranes obtained at different temperatures.

the membrane matrix and the selectivity is kept at a constant value of 4.6.

The fitting of permeabilities, sorption and diffusion coefficients according to eqs (3)–(5), respectively, are plotted in Figure 5 to quantify the effect of temperature. As expected, the CO$_2$ sorption decreases with temperature [11], while the diffusivity increases with temperature, which corresponds to the permeability decrease with temperature in Figure 5(A).

The experimental results are compared in terms of the activation energies with a previous work [5] where [emim][Ac] based SILMs were evaluated on CO$_2$/N$_2$ separation, as well as reported literature on pure CS membranes [11]. The activation energies for permeation, sorption and diffusion are given in Table 2. The activation energies for the pristine CS membranes prepared in this work agree with literature, while the introduction of RTIL in the hybrid RTIL/CS membrane decreases the permeation activation energy, leading to a lower influence of the temperature in the permeability and diffusivity. The RTIL enhances the CO$_2$ affinity of the membrane material and reduces the influence of temperature in diffusivity and, therefore, permeability. These values validate the solution-diffusion model [5, 11].

5 Conclusions

In this work, new hybrid RTIL/CS membranes were prepared from green solvent [emim][Ac] RTIL and CS, a commercial polymer obtained from natural resources. Their CO$_2$ and N$_2$ permeation, sorption and diffusion were determined at temperatures ranging from 298 to
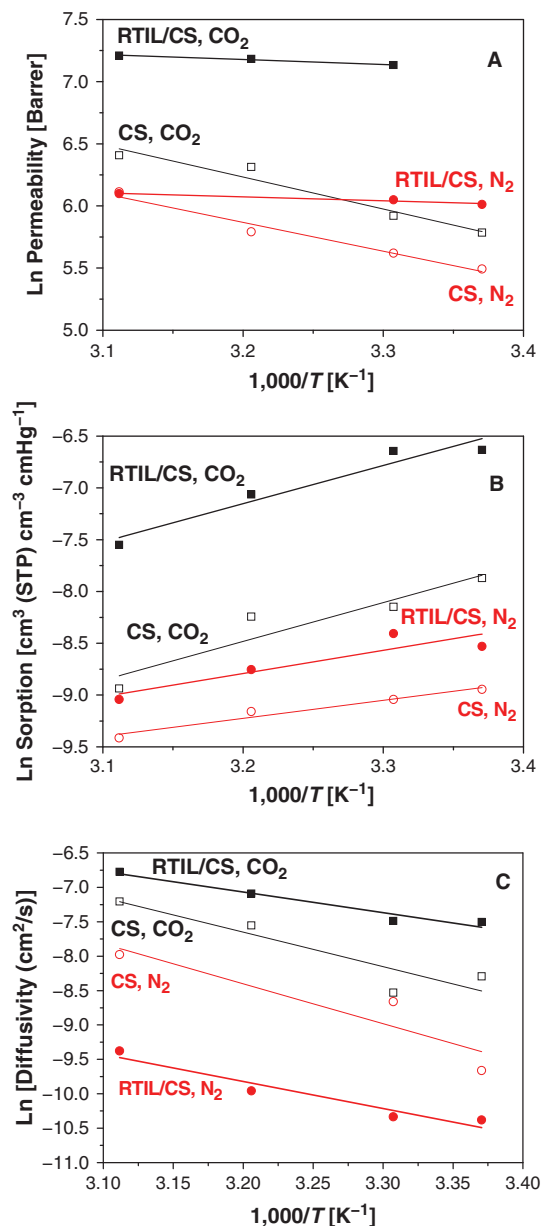

Figure 5: Permeation (A), sorption (B) and diffusion (C) of CO$_2$ and N$_2$ as a function of temperature through pure CS and hybrid RTIL/CS membranes.

Table 2: Arrhenius parameters for CO$_2$ and N$_2$ in CS and RTIL/CS membranes.

Membranes	E_P (kJ/mole)		ΔH_S (kJ/mole)		E_D (kJ/mole)	
	CO$_2$	N$_2$	CO$_2$	N$_2$	CO$_2$	N$_2$
SILMs [5]	19.4	25.3	−8.3	–	7.9	–
CS [11]	34.1	44.9	−13.6	−3.3	47.9	48.1
CS	21.4	19.3	−31.2	−14.5	41.8	48.2
RTIL/CS	3.3	2.6	−30.7	−18.6	25.0	32.7

323 K. The temperature influence was well described by the Arrhenius–van't Hoff exponential relationships. The introduction of RTIL in the hybrid RTIL/CS membrane decreases the permeation activation energy, leading to a lower influence of the temperature in the permeability and diffusivity. Moreover, the thermal behavior is similar to pure CS membranes, and the mechanical strength and flexibility were improved due to the introduction of the RTIL in the polymer matrix. Further research is being conducted on the development of hybrid membranes based on acetate-based ionic liquid, monomer and ionic polymers with large CO_2 affinity and never used in membrane technology so far.

Notation

A_m	membrane area (m^2)
D	diffusion coefficient ($cm^2 \, s^{-1}$)
D_0	pre-exponential factor of diffusion ($cm^2 \, s^{-1}$)
E_D	activation energy of diffusion ($kJ \, mol^{-1}$)
E_p	activation energy of permeation ($kJ \, mol^{-1}$)
P	gas permeability (Barrer)
P_0	pre-exponential factor of gas permeability (Barrer)
p_{feed}	pressure in the feed compartment (Pa)
p_{perm}	pressure in the permeate compartment (Pa)
R	ideal gas constant ($bar \, L \, mol^{-1} \, K^{-1}$)
S	gas adsorption ($cm^3(STP) \, cm^{-3} \, cm \, Hg^{-1}$)
S_0	pre-exponential factor of gas sorption ($cm^3(STP) \, cm^{-3} \, cm \, Hg^{-1}$)
T	temperature (K)
t	time (s)
V_{feed}	volume of the feed compartment (m^3)
V_{perm}	volume of the permeate compartment (m^3)

Greek letters

β	geometric factor (m^{-1})
δ	membrane thickness (m)
ΔH_s	heat of sorption ($kJ \, mol^{-1}$)

References

1. Rochelle GT. Amine scrubbing for CO_2 capture. Science 2009; 325:1652–4.
2. Hägg M-B. 2009. Membranes in gas separation. In: AK. Pabby, SSH. Rizvi, AM. Sastre, editors. Handbook of membrane separations. Boca Raton, FL: CRC Press, Taylor & Francis, 65–103.
3. Robeson LM. The upper bound revisited. J Membr Sci 2008; 320:390–400.
4. Seddon KR. Ionic liquids for clean technology. J Chem Tech Biotechnol 1997;68:351–6.
5. Santos E, Albo J, Irabien A. Acetate based supported ionic liquid membranes (SILMs) for CO_2 separation: influence of the temperature. J Membr Sci 2014;452:277–83.
6. Neves LA, Crespo JG, Coelhoso IM. Gas permeation in supported ionic liquid membranes. J Membr Sci 2010;357:160–17.
7. Chung T-S, Jiang LY, Li Y, Kulprathipanja S. Mixed matrix membranes (MMMs) comprising organic polymers with dispersed inorganic fillers for gas separation. Prog Pol Sci 2007;32:483–507.
8. Dong Y, Wang M, Chen L, Li M. Preparation, characterization of P(VDF-HFP)/[bmim]BF_4 ionic liquids hybrid membranes and their pervaporation performance for ethyl acetate recovery from water. Desal 2012;295:53–60.
9. Hao L, Li P, Yang T, Chung T-S. Room temperature ionic liquid/ ZIF-8 mixed-matrix membranes for natural gas sweetening and post-combustion CO_2 capture. J Membr Sci 2013;436:221–31.
10. Hudiono YC, Carlisle TK, Bara JE, Zhang Y, Gin DL, Noble RD. A three-component mixed-matrix membrane with enhanced CO_2 separation properties based on zeolites and ionic liquid materials. J Membr Sci 2010;350:117–23.
11. El-Azzami LA, Grulke EA. Dual mode model for mixed gas permeation of CO_2, H_2, and N_2 through a dry chitosan membrane. J Polym Sci B 2007;45:2620–31.
12. Casado-Coterillo C, Andrés F, Téllez C, Coronas J, Irabien A. Synthesis and characterization of ETS-10/chitosan nanocomposite materials for pervaporation. Sep Sci Technol 2014;49:1903–9.
13. Casado-Coterillo C, López-Guerrero MD, Irabien A. Synthesis and characterisation of ETS-10/acetate-based ionic liquid/chitosan mixed matrix membranes for CO_2/N_2 separation. Membranes 2014;4:287–301.
14. Albo J, Santos E, Neves LA, Simeonov SP, Afonso CA, Crespo JP, et al. Separation performance of CO_2 through supported magnetic ionic liquid membranes (SMILMs). Sep Purif Technol 2012;97:26–33.
15. Bara JE, Lessmann S, Gabriel CJ, Hatakeyama ES, Noble RD, Gin DL. Synthesis and performance of polymerizable room-temperature ionic liquids as gas separation membranes. Ind Eng Chem Res 2007;46:5397–404.
16. Cussler EL. Diffusion. Mass transfer in fluid systems. 2nd ed. New York: Cambridge University Press, 1997:21–23, 434–5, 438–9.
17. Crank J. The mathematics of diffusion. 2nd ed. Oxford: Clarendon Press, 1975: 411.
18. Zuo G, Wan Y, Wang L, Liu C, He F, Luo H. Synthesis and characterization of laminated hydroxyapatite/chitosan nanocomposites. Mater Lett 2010;64:2126–8.
19. Xu D, Loo LS, Wang K. Characterization and diffusion behavior of chitosan-POSS composite membranes. J Appl Pol Sci 2011;122:427–35.
20. Liu Y, Yu S, Wu H, Li Y, Wang S, Tian Z. High permeability hydrogel membranes of chitosan/poly ether-block-amide blends for CO_2 separation. J Membr Sci 2014;469:198–208.
21. Balau L, Lisa G, Popa MI, Tura V, Melnig V. Physico-chemical properties of chitosan films. Cent Eur J Chem 2004;2:638–47.
22. El-Azzami LA, Grulke EA. Carbon dioxide separation from hydrogen and nitrogen by fixed facilitated transport in swollen chitosan membranes. J Membr Sci 2008;323:225–34.